J. Physiol. (1981), **312**, *pp.* 471–490
With 11 *text-figures*
Printed in Great Britain

ANALYSIS OF SUBTHRESHOLD PACE-MAKER CURRENTS IN CHICK EMBRYONIC HEART CELLS

BY JOHN R. CLAY* AND ALVIN SHRIER†
From the Department of Anatomy, Emory University, Atlanta, GA 30322, U.S.A.

(*Received 21 April 1980*)

SUMMARY

1. Small re-aggregates of cells dissociated from the ventricles of 7-day-old chick embryonic hearts beat spontaneously in low external potassium concentration (K_o = 1·3 mM) tissue culture medium. This activity was blocked by the addition of tetrodotoxin (TTX) or potassium ions to the external medium.

2. A two-micro-electrode voltage-clamp technique was used to analyse the subthreshold currents responsible for the pace-maker depolarization.

3. Voltage-clamp steps 6–10 sec in duration revealed a time-dependent current having first order kinetics. Its membrane potential range of steady-state activation was −90 to −60 mV.

4. The current kinetics were qualitatively similar to those of Hodgkin & Huxley (1952*b*) with a peak time constant of approximately 1 sec at $V = -75$ mV. The kinetics were independent of K_o.

5. The time-dependent current was attributed to gated membrane channels. The fully activated current–voltage (I–V) relation of the channels was determined from the ratio of the amplitudes of the time-dependent currents during and after voltage-clamp steps following the procedure of Noble & Tsien (1968).

6. The fully activated I–V relation displayed inward rectification with negative slope conductance at potentials more than 15 mV positive to its reversal potential. Changes of K_o shifted the I–V curve along the voltage axis like a potassium electrode.

7. The time-independent (background) current was obtained by subtracting the gated channel current from the steady-state I–V curve. This current also rectified in the inward direction.

8. The inwardly rectifying I–V relations were theoretically described by a channel having a row of ion-selective sites along which ions move in a single file (Hodgkin & Keynes, 1955), and a membrane-bound particle which blocked the channel in a voltage-dependent manner.

9. The relationship of the voltage-clamp results to spontaneous activity is discussed and comparisons are made with measurements from whole embryonic heart and other cardiac tissues.

* Present address: Laboratory of Biophysics, NIH, NINCDS, Marine Biological Laboratory, Woods Hole, MA 02543, U.S.A.

† Present address: Department of Physiology, McGill University, Montreal, PQ H3G 1Y6, Canada.

0022-3751/81/3890-0933 $07.50

INTRODUCTION

The first visible contraction of the embryonic vertebrate heart occurs at an early stage of development, soon after the primitive ventricle has formed (Sabin, 1917; Johnstone, 1925; Patten & Kramer, 1933; Barry, 1942). The electrical pace-maker for the initial beat in the chick embryo is located in the primitive sino-atrial region (Van Mierop, 1967). Spontaneous beating also occurs in muscle fragments, individual cells and re-aggregates of cells which are isolated from the heart ventricles or atria of chick embryos incubated for 2–7 days. The beat rates are characteristic of the region of the heart from which the cells are taken (Barry, 1942; Cavanaugh, 1955; DeHaan, 1970; Sachs & DeHaan, 1973). However, ventricle and atrial preparations lose their automaticity during the last 2 weeks of incubation from day 7 onward to day 21, when the chick hatches (DeHaan, 1970; Sachs & DeHaan, 1973).

In this paper we report voltage-clamp measurements of some of the time-and voltage-dependent membrane currents which underlie automaticity in re-aggregates of dissociated 7-day embryonic ventricular cells. We report developmental changes of these currents in the subsequent paper (Clay & Shrier, 1981) based on voltage-clamp measurements from ventricular cell aggregates prepared from chick embryos incubated for 12 or 17 days.

A brief description of some of our results has been published (Shrier & Clay, 1980).

METHODS

Preparation

The apical portions of heart ventricles were dissected from White Leghorn chick embryos incubated at 37 °C for 7 days. The tissue was dissociated into its component cells in 0·05 % trypsin (1:300, Nutritional Biochemical Co.) by the multiple-cycle trypsinization process described elsewhere (DeHaan, 1967, 1970). This procedure yields a suspension that is 85–90 % single cells. An inoculum of 5×10^5 cells was added to 3 ml. of culture medium 818A (DeHaan, 1970) contained in a 25 ml. Erlenmeyer flask. The flask was gassed with 5 % CO_2, 10 % O_2, 85 % N_2,sealed with a silicone rubber stopper, and placed on a gyratory shaker (62 rev/min, $1\frac{1}{4}$ in. stroke) for 48–72 hr at 37 °C to allow spherical aggregates to form (Sachs & DeHaan, 1973). The contents of each flask were transferred to a plastic tissue culture dish on the warm stage of a dissecting microscope. The aggregates adhered firmly to the bottom of the dish in an hour or less. The temperature was maintained at 37 °C (continuously monitored) and the gas mixture was passed through a toroidal gassing ring surrounding the top of the dish. Non-toxic mineral oil layered over the medium prevented evaporation while providing an unclouded view of the cells. These conditions maintained the dish at a constant atmosphere and a pH of 7·3.

Medium 818A contains (by volume) 25 % M199 (Grand Island Biological Co., Grand Island, N.Y.), 2 % heat-inactivated selected horse serum (K.C. Biologicals, Lenexa, Kansas), 4 % fetal calf serum (Grand Island) and 0·5 % gentamycin (Schering Corp., Bloomfield, N.J.) in K-free Earle's balanced salt solution which contains (mM): NaCl, 116·0; $MgSO_4$, 0·8; NaH_2PO_4, 0·9; $CaCl_2$, 1·8; $NaHCO_3$, 26·2; glucose, 5·5. The potassium concentration of the final medium was adjusted to one of five levels: 1·3, 2·5, 3·5, 4·8 or 6 mM. Tetrodotoxin (TTX; Sigma) was added to the tissue culture dish at a concentration of 3 μM to suppress spontaneous activity.

The range of diameters (D) of heart cell aggregates prepared from 48–72 hr gyration culture conditions was typically 100–300 μm. The number of cells (N) and the total amount of membrane surface area (A) in an aggregate could be estimated from its volume ($\pi D^3/6$), the single cell diameter $d = 10{\cdot}8$ μm (B. Atherton & R. L. DeHaan, unpublished) and the amount of extracellular space in an aggregate, which has been estimated at 4 % (Clapham, 1979). Combining all of these factors gives $N = 6170$ cells and $A = 2{\cdot}15 \times 10^{-2}$ cm^2 membrane surface area for $D = 200$ μm, which is the size of preparation from which most of our measurements have been made.

Electrophysiology

Spontaneous action potentials and membrane currents during voltage clamp were measured with two glass micro-electrodes containing 3 M-KCl which were impaled within two different cells, widely spaced in the aggregate. Electrode resistance was typically 20–50 MΩ. Standard voltage-clamp circuitry was used (Connor & Stevens, 1971) with a Model 171K (Analog Devices; Norwood, Mass.) operational amplifier. Current was recorded from the voltage drop across a 10 MΩ feed-back resistor of a second operational amplifier (Analog Devices, Model 48K) which held the bathing medium at virtual ground via an agar salt bridge and an Ag:AgCl wire. Membrane current in response to rectangular voltage-clamp steps was recorded on FM magnetic tape at $3\frac{3}{4}$ in/sec (DC – 625 Hz) for off-line analysis.

Data analysis

Time constants and amplitudes of membrane currents were determined from photographs of oscilloscope traces of the experimental records with a Hewlett Packard (Beaverton, Ore.) 9810A calculator, 9864A digitizer and 9862 plotter. The currents were routinely filtered (Kron-Hite Model 332, Avon, Mass., in low-pass mode, 3db cut-off at 50 Hz), although frequent comparisons were made before and after this procedure to ensure that it did not produce an error in the time-constant determination.

Theoretical model of inward rectification

The experimentally obtained I–V relations were modelled by knock-on single-file diffusion of ions through narrow pores or channels containing some number of ion-selective sites (Hodgkin & Keynes, 1955). The model also assumes a hypothetical blocking particle which is located either at a site on the inner surface of the membrane or within the channel at one of the ion-selective sites (Cleemann & Morad, 1979). The blocker is knocked into the channel by collisions of permeant ions from either side of the membrane. That is, some fraction, β, of all collisions with the channel knocks the blocker loose. The probability that it then enters the channel depends upon the membrane potential level (V) with respect to the equilibrium potential E_{eq}. If $V \gg E_{eq}$, it will almost certainly enter the channel: if $V \ll E_{eq}$, it almost certainly will not. We let this probability be p_+ which is also the probability that the row of ions and blocker moves outward with each collision when the blocker is inside the channel. We let the average interval between collisions be $\bar{t}$. Consequently, the probability that the blocker enters the channel in the interval $(t, t+\mathrm{d}t)$ is $\beta p_+ \mathrm{d}t/\bar{t}$, given that it was at its site on the inner surface at time t. The probability that the blocker moves further outward is $(1-\beta)p_+\mathrm{d}t/\bar{t}$, except when it is located at the outermost site, where it has zero probability of outward movement. Inward movement is treated in a similar manner with the quantity p_+ replaced by p_-. With these assumptions the net membrane current is given by (J. R. Clay & M. F. Shlesinger, unpublished calculations):

$$I = Ne\bar{t}^{-1}(1-\beta)^2\beta^{-1}(p_-/p_+)^r(p_+-p_-)/(1+p_-/p_+ + (p_-/p_+)^2 + \ldots + (p_-/p_+)^{r-1} + (1-\beta)(p_-/p_+)^r/\beta),\ \mathrm{r} = 1,2,3\ldots, \quad (1)$$

where N is the channel density, e is the electronic charge, r is the number of channel sites, and (Clay & Shlesinger, 1977)

$$p_+ = (1+\exp(-\mathrm{e}(V-E_{eq})/k_BT))^{-1}, \quad p_+ + p_- = 1, \quad (2)$$

where k_B is the Boltzmann constant ($-e$(T is the absolute temperature.

Application of voltage clamp to aggregates

The heart-cell aggregate is suitable for a voltage-clamp analysis of membrane currents in the pace-maker voltage range, because the cells in these preparations are well coupled (DeHaan & Fozzard, 1975; DeFelice & DeHaan, 1977), the spherical geometry is optimal for minimizing the influence of the distributed series resistance, the extracellular cleft spaces are relatively large and uniformly distributed throughout the aggregate (Clapham, 1979) and the amplitudes of pace-maker currents are small compared to those which flow during an action potential. The evidence for coupling is based on electrophysiological measurements of small signal impedance and membrane voltage noise from quiescent aggregates. These results indicate that the coupling ratio for the electrical potential within any two cells is virtually unity for low-frequency signals ($f \lesssim 100$ Hz) (DeFelice & DeHaan, 1977; Clay, DeFelice & DeHaan, 1979). The spherical geometry is favourable

because a majority of the cells are in the outermost layers of the preparation. For example, approximately 65 % are in the three outermost layers for a $D = 200$ μm preparation. Consequently, the cleft spaces near these cells are close to the medium outside the aggregate. The relative volume of these spaces is $3{\cdot}7 \pm 2{\cdot}0$ % (Clapham, 1979). By comparison, the volume of distributed extracellular space in cardiac Purkinje fibre is approximately 1 % (Hellam & Studt, 1974).

Finally, the amplitude of the currents which we have measured is less than 40 nA, which corresponds to a density of approximately 2 μA/cm^2. By comparison, the peak inward sodium current is approximately 200 μA/cm^2 (Nathan & DeHaan, 1979). We note that 2 μA/cm^2 is also small compared with potassium currents in nerve, which are of the order of 1–10 mA/cm^2 both in non-myelinated nerve axons (Hodgkin & Huxley, 1952*a*) and in the node of Ranvier of myelinated axons, using 50 μm^2 for the area of the nodal membrane (Hille, 1973; Tasaki, 1955).

The electrophysiological evidence which suggests that the series resistance is negligible for our measurements is that the input capacitance (C_i) determined from the initial slope of the voltage response to current steps is proportional to D^3, and the steady-state input slope resistance (R_i) at constant potential is inversely proportional to D^3 (Clay *et al.* 1979). Since the total membrane surface area (A) is also proportional to D^3, the size dependence of R_i and C_i, together with the internal isopotentiality, indicate that a lumped circuit model of the aggregate in which series resistance is neglected is appropriate for step-clamp measurements in the pace-maker voltage range. Further evidence for this view is given in the Discussion.

RESULTS

Spontaneous activity

Virtually all aggregates prepared from the ventricles of 7-day-old embryos beat spontaneously and rhythmically in tissue culture medium containing 1·3 mM-potassium with a beat rate of 120–150 beats/min for a 100 μm aggregate. The rate diminished with increasing size, as shown previously by Sachs & DeHaan (1973). An intracellular recording of action potentials and spontaneous pace-maker depolarization for a $D = 120$ μm aggregate is shown in Fig. 1. The pooled results for the action potential parameters from several different preparations were 161 ± 15 msec for its duration (a.p.d.), -88 ± 5 mV for the maximum diastolic potential (m.d.p.), 28 ± 2 mV for the overshoot potential (o.s.), and 155 ± 37 V/sec for the maximum rate of rise ($\dot{V}_{max}$) ($n = 5$, $\pm$S.D.). These parameters were not markedly influenced by size of the aggregates in the $D = 100$–250 μm range. Application of 3 μM-TTX usually blocked spontaneous activity although occasional periods of beating lasting 30–60 sec were observed in a few preparations. The resting potential of quiescent aggregates was -56 ± 7 mV ($n = 11$). Approximately 1 nA of depolarizing current was sufficient to induce continuous, rhythmic beating in a 100 μm diameter TTX-treated aggregate. Slightly larger currents were required to induce beating in larger preparations. The parameters of either the induced or the spontaneous action potentials from the TTX-treated preparations were m.d.p. $= -92 \pm 3$ mV, o.s. $= 33 \pm 4$ mV, a.p.d. $= 165 \pm 10$ msec, and $\dot{V}_{max} = 14 \pm 2$ V/sec ($n = 9$). The only statistically significant change in the action potential parameters produced by TTX was a reduction of $\dot{V}_{max}$ to about one-tenth of its control value. Elevation of external potassium concentration (K_o) also blocked or reduced spontaneous activity. Irregular beating with a mean rate of 5–10 beats/min was observed with $K_o = 2{\cdot}5$ mM. Spontaneous beating was rarely observed with $K_o = 3{\cdot}5$–6 mM. The resting potential under these conditions was -78 ± 3 mV ($n = 16$) and appeared to be unmodified by the application of 3 μM-TTX.

Steady-state current–voltage (I–V) relations

The steady state current voltage (I–V) relations for various levels of K_o are shown in Fig. 2. The results for K_o = 2·5, 4·8 and 6 mM are from a continuous impalement of a single aggregate. The I–V relation for K_o = 1·3 mM is a representative result from a different preparation of comparable size (D = 200 μm). As shown in Fig. 2, the primary effects of elevating K_o from 1·3 mM were to shift in $I-V$ relation in the outward current direction and to introduce a region of negative slope conductance in the −70 to −50 mV potential range.

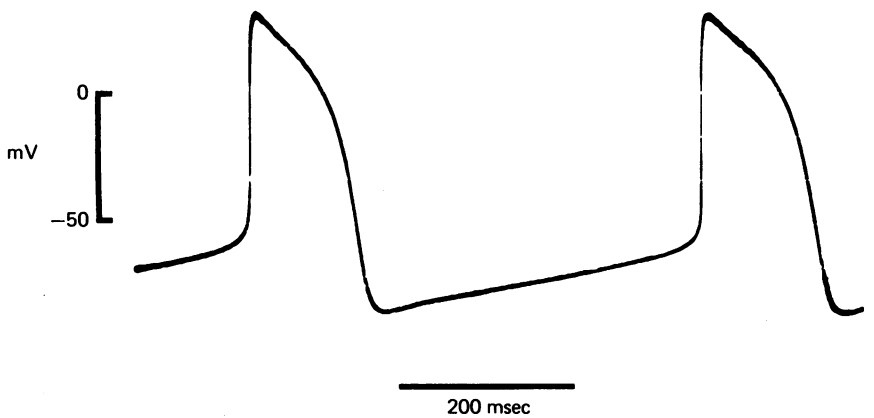

Fig. 1. Action potentials and intervening pace-maker depolarization from a 7-day aggregate (D = 120 μm) in K_o = 1·3 mM.

Time-dependent currents

The 7-day aggregate contained a time-dependent current which did not inactivate, as shown by the responses to 10 sec voltage-clamp steps in Fig. 3 (holding potential, V_H = −79 mV; K_o = 2·5 mM). The time-dependent changes were described by single exponential functions of time, with a time constant which depended upon the potential of the step (Fig. 4). The time constants of the currents which occurred when the voltage was stepped back to the holding potential (I_b in Fig. 3) were all approximately the same, even though the amplitudes of these currents were all different. These results indicated that the kinetics were qualitatively similar to those which Hodgkin & Huxley (1952*b*) described in squid giant axon. That is, the time constant τ_s was solely a function of the membrane potential and was independent of the past history of the preparation for the simple clamp protocol in Fig. 3. Moreover, τ_s was a bell-shaped function (Fig. 5*A*), and the amplitude of the I_b current was a sigmoidal function of potential (Fig. 5*B*). The continuous line in Fig. 5*A* is the best fit to the τ_s data of $(\alpha+\beta)^{-1}$ and the continuous line in Fig. 5*B* is the corresponding fit to the normalized I_b currents of $\alpha/(\alpha+\beta)$ (Hodgkin & Huxley, 1952*b*; McAllister, Noble & Tsien, 1975), where

$$\alpha = \alpha_0(V-V_1)/(1-\exp(-\alpha_1(V-V_1))) \quad (3)$$

and

$$\beta = \beta_0 \exp(-\beta_1(V-V_1)). \quad (4)$$

The best fit values of the parameters α_0, β_0, α_1, β_1 and V_1 for the preparation described in Figs. 3–5 and all other experiments are given in the legend of Table 1.

The step-clamp results indicated that only a single time-dependent current was present in the −60 to −120 mV range. Its analysis was aided by theoretically ascribing it to ion flow through membrane channels, each of which was gated by a particle or a membrane subunit that was either open, thereby allowing ions to flow, or closed, thereby blocking ion flow (Neher & Stevens, 1977). More than one gating

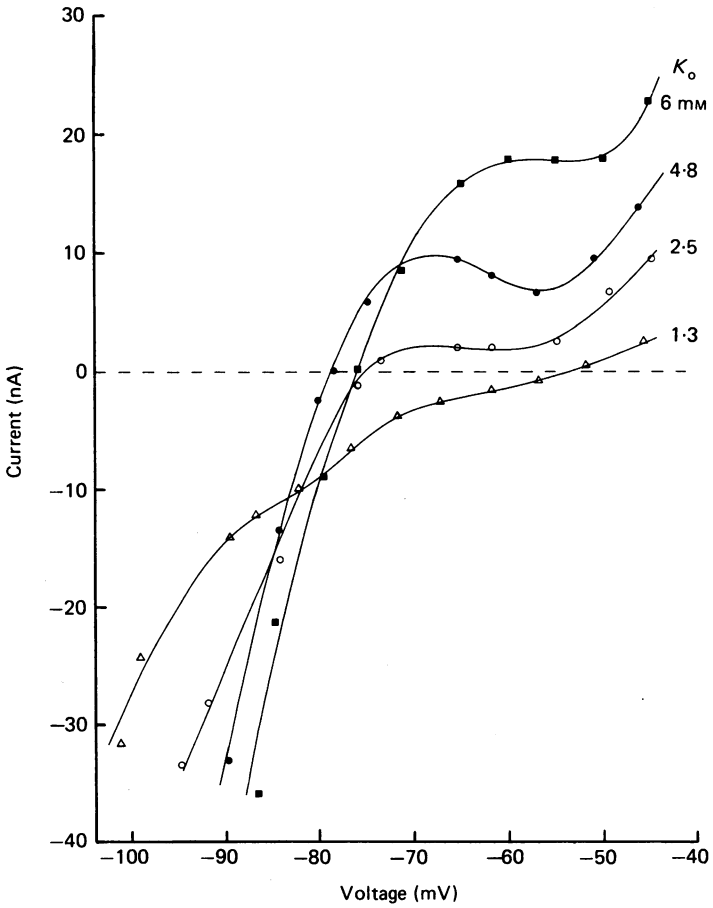

Fig. 2. Steady-state I–V relations from 7-day aggregates in 3 μM-TTX as a function of K_o. The results for K_o = 2·5, 4·8 and 6 mM are from a continuous impalement of a single preparation (D = 200 μm). The relation for K_o = 1·3 mM is a representative result from a different aggregate of comparable size. The current measurements were made either at the end of 10 sec clamp steps or during steady holding potential conditions. Lines drawn through the points by eye.

particle per channel may be involved, as hypothesized for nerve membrane (Hodgkin & Huxley, 1952*b*; Stevens, 1972). However, the fact that the time-dependent changes, such as those in Fig. 3, were exponential, rather than sigmoidal functions of time, suggested that a model with a single gating particle was appropriate.

The gate of any one channel was assumed to be open at some arbitrary time t and voltage V with probability $s(V,t)$, which we represent as $s_\infty(V_H)$ for steady-state

voltage-clamp conditions. During a clamp step, $s(V,t)$ changes with an exponential time course until its new steady-state value $s_\infty(V_{step})$ has been reached. This behaviour is described (Hodgkin & Huxley, 1952*b*) by

$$ds(V,t)/dt = -s(V,t)/\tau_s + \alpha. \quad (5)$$

The current amplitude is given by $I(t) = N_s s(V,t) i(V)$, where N_s is the density of channels, either open or closed, and $i(V)$ is the current–voltage relation for ion flow

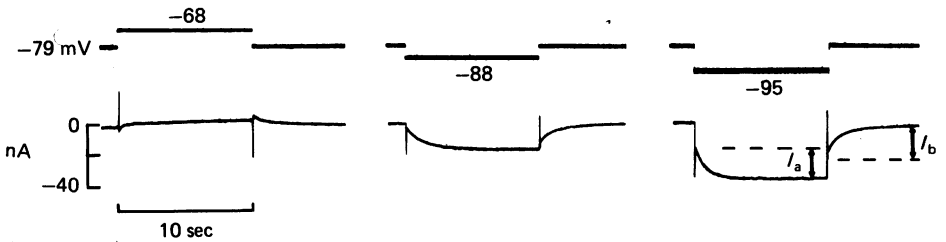

Fig. 3. Step-clamp records of an aggregate in K_o = 2·5 mM (D = 200 μm). V_H = −79 mV. Voltage stepped to levels shown. I_a and I_b, as shown for example in the right-hand panel, represent amplitudes of the time-dependent currents during and after the clamp step. Records are filtered (low pass; 3db roll-off at 50 Hz). Settling time of voltage control was 5–15 msec.

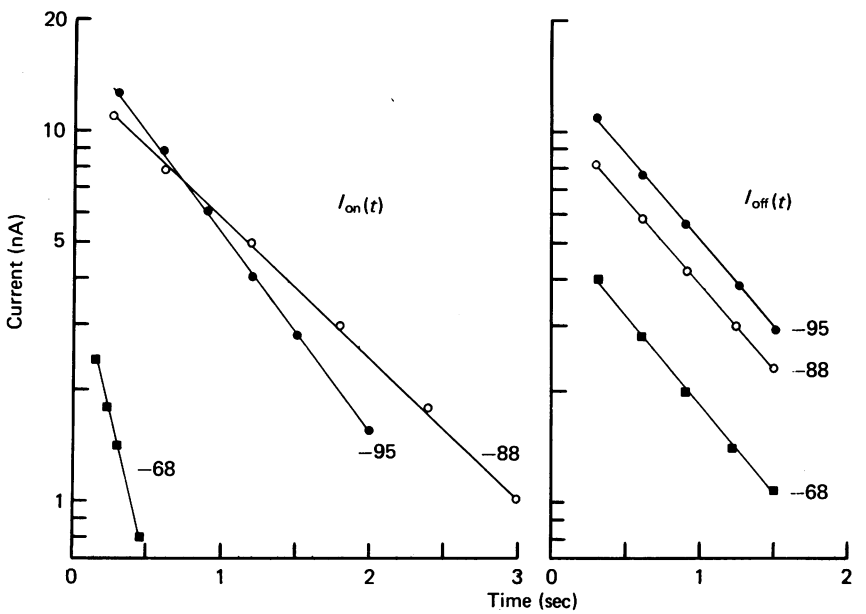

Fig. 4. Semilogarithmic plots of time-dependent currents in Fig. 3. $I_{on}(t)$ represents the time course of current change with reference to the steady current level at the end of the step. The amplitude of I_{on} at t = 0 is I_a. Similarly, $I_{off}(t)$ represents the time course of current change with reference to the steady holding current after V was stepped back to V_H = −79 mV ($I_{off}(0) = I_b$). The number alongside each set of points is the potential to which the membrane was clamped during the voltage step. The absolute value of current is plotted so that the responses to both depolarizing and hyperpolarizing clamp steps could be plotted on the same scale. The straight lines were drawn through the points by eye. The time constant, τ_s, of $I_{on}(t)$ is 0·25 sec for V_{step} = −68 mV, 1·07 sec for V_{step} = −88 mV, and 0·79 sec for V_{step} = −95 mV. The τ_s for $I_{off}(t)$ is 0·90–0·96 sec.

through a single channel. For unmyelinated nerve axon channels $i(V)$ is $\gamma(V-E_{eq})$, where γ is the single channel conductance and E_{eq} is the equilibrium potential for the ions which pass through the channel. In general $i(V)$ is not a linear function of the driving force. For example, channels in myelinated nerve axons are described by the Goldman–Hodgkin–Katz current–voltage relation, which is a non-linear

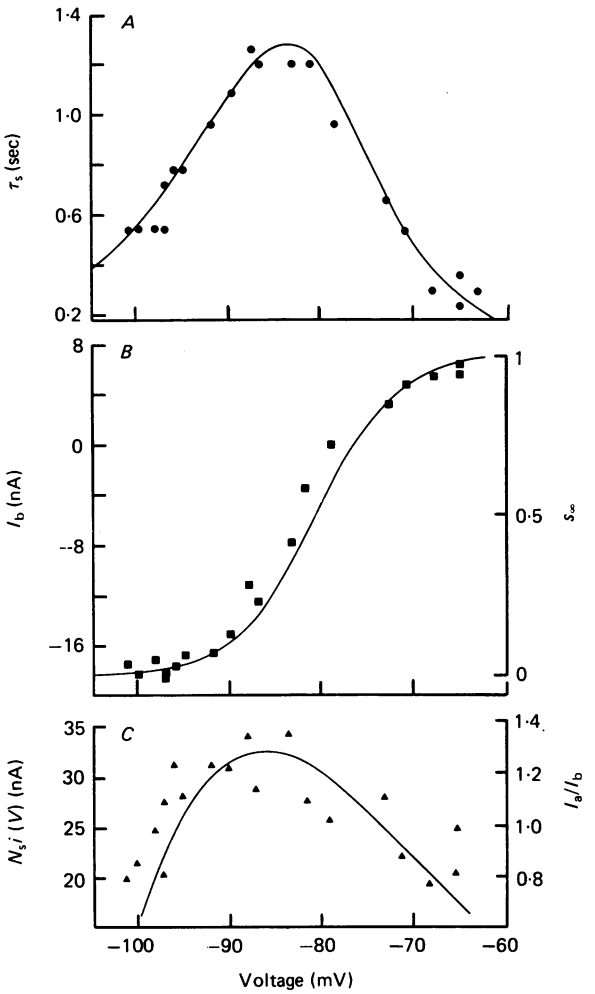

Fig. 5. Kinetics and rectifier properties of the time-dependent current. Same preparation as in Fig. 3 (K_o = 2·5 mM). *A*, time constant, τ_s, of current changes in response to voltage steps. Continuous line is best fitted by eye to these data of the function $(\alpha+\beta)^{-1}$, where $\alpha = \alpha_0(V-V_1)/1-\exp(-\alpha_1(V-V_1)))$, and $\beta = \beta_0 \exp(-\beta_1(V-V_1))$. The best fit values of the parameters in these expressions are α_0 = 1·05 sec^{-1}, β_0 = 0·095 sec^{-1}, α_1 = 0·2 mV^{-1}, β_1 = 0·075 mV^{-1} and V_1 = −61 mV. *B*, amplitude of I_b currents. Right-hand scale represents the normalized I_b currents. Continuous line represents $s_\infty = \alpha/(\alpha+\beta)$. *C*, fully activated current ($N_s i(V)$) of the gated channels, as determined by the ratio analysis. For each clamp record I_a/I_b (right-hand scale) was determined and plotted on this graph at $V = V_{step}$. $N_s i(V)$ was obtained by multiplying each point by the full distribution of I_b currents in *B* which is approximately 27 nA. Continuous line is the best fit to the Clay and Shlesinger model of inward rectification described by data of eqns. (1) and (2) with $N_s e/\tilde{t}$ = 1·36 μA, r = 2, and β = 0·5.

TABLE 1. Properties of time-dependent I_{K_2} current in 7-day aggregates*

Preparation	K_o (mM)	Voltage at which maximum time constant occurred† (mV)	(I_p) Maximum outward current‡ (nA)	Voltage at which I_p occurred‡ (mV)
2-20-78	1·3	−76	24·5§	−107§
5-17-78	4·8	−81	22·2	−73
6-18-78	2·5	−76	24·0	−81
7-05-78	2·5	−82	21·4	−90
2-01-79	3·5	−76	26·4	−76
4-02-79	2·5	−80	29·6	−89
4-02-79	3·5	−80	25·8	−79
4-02-79	4·8	−80	20·9	−71
4-18-79	2·5	−84	26·2	−89
4-19-79	2·5	−84	32·5	−86
4-19-79	3·5	−84	27·7	−78
5-04-79	3·5	−83	22·6	−79
5-06-79	3·5	−86	34·0	−82
5-14-79	1·3	−76	27·0§	−95§
5-24-79	1·3	−78	32·4§	−100§

* Range of diameters of aggregates was 180–220 μm.

† As determined from the fit to the time constant data of $\tau_s = (\alpha+\beta)^{-1}$, where $\alpha = \alpha_0(V-V_1)/(1-\exp(-\alpha_1(V-V_1)))$ and $\beta = \beta_0 \exp(-\beta_1(V-V_1))$. The best-fit representation of all the data corresponded to $\alpha_0 = 1{\cdot}05$ sec^{-1}, $\beta_0 = 0{\cdot}095$ sec^{-1}, $\alpha_0 = 0{\cdot}2$ mV^{-1}, $\beta_1 = 0{\cdot}075$ mV^{-1}. The peak value of τ_s is 1·28 sec, which occurs at $V = V_1 - 23$ mV. That is, V_1 is equal to the number in the third column plus 23 mV.

‡ As determined from the best fit of eqns. (1) and (2) to the fully activated I–V relation with $r = 2$ and $\beta = 0{\cdot}5$.

§ Extrapolated from the best fit of eqns. (1) and (2) to the fully activated I–V relation.

function of $(V-E_{eq})$ (Goldman, 1943; Hodgkin & Katz, 1949; Frankenhauser, 1962). We do not know, *a priori*, what $i(V)$ is for the current described in Figs. 3 and 4. A further complication is that current from a second type of channel, which is not gated, may also be present. We represent this time-independent, or background, current as $I_{bg}(V) = N_{bg} i_{bg}(V)$, where $i_{bg}(V)$ is the current–voltage relation of these channels. In general, $i_{bg}(V)$ is different from $i(V)$. Moreover, one or more types of non-gated currents may be present. However, they may all be lumped together in the I_{bg} term in an analysis of the time-dependent current.

In general $I_{bg}(V)$ is a non-linear function of V, as is $I(V,t)$. Consequently, a simple subtraction of $I_{bg}(V)$ from the records in Fig. 3 is not appropriate. An alternative approach was provided by Noble & Tsien (1968), who showed that both $I_{bg}(V)$ and $I(V,t)$ can be determined from step records by taking advantage of the fact that the time course of i_{bg}, and hence I_{bg}, after a step is made is at least one or two orders of magnitude faster than $s(V,t)$. Consequently, it does not contribute to the measured time-dependent changes I_a and I_b (Fig. 3, right-hand panel). Similarly, $i(V)$ equilibrates to its new level almost instantaneously. Consequently, the net membrane current $I(V, t)$, after V is clamped to V_{step} is initially given by

$$I(V_{step};\, t=0) = N_s s_\infty(V_H) i(V_{step}) + I_{bg}(V_{step}). \qquad (6)$$

If the duration of the step (t_{step}) is much greater than the time constant of the current change, as in Fig. 3, the current at the end of the step will be the same as that which would flow if the potential were held at V_{step} in the steady state. That is,

$$I(V_{step}, t = t_{step}) = N_s s_\infty(V_{step}) i(V_{step}) + I_{bg}(V_{step}). \quad (7)$$

The amplitude of the time-dependent current change during the clamp step, I_a, is the difference between eqns. (6) and (7). That is,

$$I_a = N_s i(V_{step})(s_\infty(V_H) - s_\infty(V_{step})). \quad (8)$$

A similar analysis gives the time-dependent current, I_b, when the voltage is stepped back to V_H. This result is

$$I_b = N_s i(V_H)(s_\infty(V_H) - s_\infty(V_{step})). \quad (9)$$

The point of this approach is that the ratio I_a/I_b is equal to $i(V_{step})/i(V_H)$, as shown by eqns. (8) and (9), which is independent of both the background current and the parameter $s(V, t)$. That is, the ratio analysis gives the voltage dependence of $i(V)$ from a series of clamp steps from a given holding potential. The results of this analysis for the preparation of Fig. 3 are shown in Fig. 5*C* (right-hand scale).

The open channel current for all of the N_s gated channels can be determined from the I_a/I_b ratio and the full distribution of I_b currents in Fig. 5*B*. The maximum I_b current in the depolarizing direction is

$$I_b^{dep}(max) = N_s i(V_H)(s_\infty(\max) - s_\infty(V_H)), \quad (10)$$

and the minimum (most negative) I_b current in the hyperpolarizing direction is

$$I_b^{hyp}(min) = N_s i(V_H)(s_\infty(\min) - s_\infty(V_H)). \quad (11)$$

The parameter s_∞ is unity for maximal depolarizing potentials, zero for maximal hyperpolarizing potentials.

The result of the ratio analysis would be the same if $s_\infty = 1$ at maximal hyperpolarizing potentials. However, the instantaneous current changes together with the steady-state *I–V* relation, especially at K_o = 1·3 mM (Shrier & Clay, 1980), indicate that this alternative scheme is incorrect and that $s_\infty = 1$ in the maximal depolarizing direction.

Consequently, the difference between eqns. (10) and (11), which is the full distribution of I_b currents, is $N_s i(V_H)$. This quantity is approximately 27 nA for the I_b currents in Fig. 5*B*. The product of $N_s i(V_H)$ and I_a/I_b gives $N_s i(V_{step})$ which corresponds to the left-hand scale of Fig. 5*C*. The continuous line in Fig. 5*C* is the best fit to the data of the model of $i(V)$ given by eqns. (1) and (2).

The results of the ratio analysis together with the kinetics described in Figs. 3–5 give a complete description of the time-dependent current. Since it is similar to the I_{K_2} pace-maker current in mammalian Purkinje fibre (Noble & Tsien, 1968) (see Discussion), we will use $I_{K_2}(V, t)$ to describe it throughout the rest of this paper with $i_{K_2}(V)$ in place of $i(V)$.

As shown in Fig. 5*C*, i_{K_2} with K_o = 2·5 mM displayed inward going, or anomalous rectification (Katz, 1949; Adrian & Freygang, 1962; Noble & Tsien, 1968), with a region of negative slope conductance positive to −90 mV. At potentials negative to −90 mV, the voltage dependence of the current was suggestive of an equilibrium

potential (E_{eq}) at about −110 mV. If this hypothesis is true, the time-dependent current should vanish when $V_{step} = E_{eq}$. This result is demonstrated by the set of records in Fig. 6 from a different preparation (K_o = 3·5 mM). These records also indicated that potassium ion accumulation did not occur to a significant, or observable, extent in our measurements of I_{K_2} kinetics (Discussion). Similar measurements of E_{eq} were made from this aggregate in K_o = 2·5 mM (−107 mV, extrapolated), 4·8 mM (−89 mV) and 6 mM (−82 mV). These results for E_{eq} *vs.* K_o gave a best fit slope of −63·5±7 mV per decade change of K_o, as compared with −61 mV, which would be expected if I_{K_2} were purely a potassium ion current. The range of internal potassium ion concentrations (K_i) which is consistent with these results is 120–140 mM, as compared with direct measurements of 151 mM for whole 7-day hearts (Carmeliet, Horres, Lieberman & Vereecke, 1976) and 146 mM for 7-day aggregates (McDonald & DeHaan, 1973).

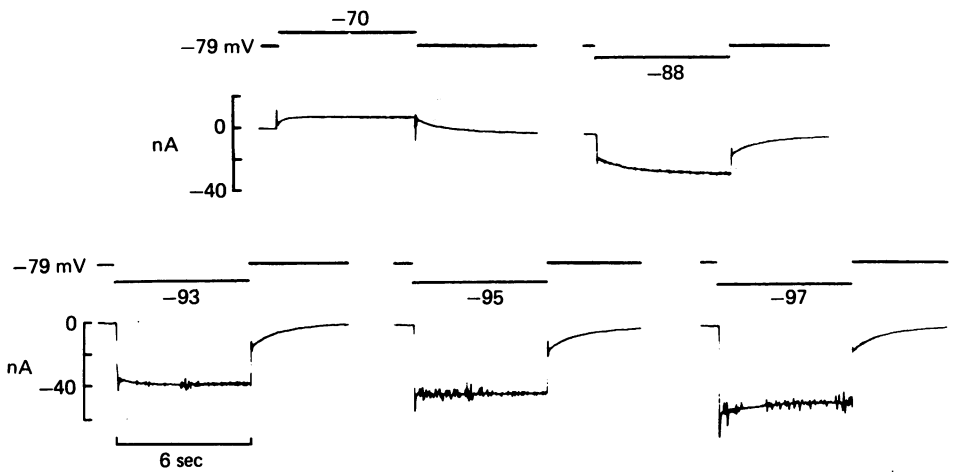

Fig. 6. Equilibrium potential of time-dependent current. Same preparation as in Fig. 2. V_H = −79 mV. V_{step} as indicated. Records are filtered (low pass; 3db roll-off at 30 Hz). K_o = 3·5 mM.

The membrane-current time constants did not appear to be a function of K_o, as shown in Fig. 7 and Table 1. Furthermore, the peak outward current ($I_p \simeq 27$ nA) was approximately the same for K_o = 2·5, 3·5 and 4·8 mM (Table 1 and Fig. 8) and the slope conductance at $V = E_K$ also appeared to be independent of K_o (Fig. 8). However, the position of i_{K_2} on the voltage axis was influenced by K_o, as shown in Fig. 8; the entire relation was shifted along the voltage axis by changes in E_K. The continuous lines in Fig. 8 are best fits of the model of inward rectification given in eqns (1) and (2).

A second time-dependent current with slow kinetics, which we label I_x, was present at potentials positive to −55 mV, as shown in Fig. 9 (V_H = −52 mV, K_o = 2·5 mM). All of the records in Fig. 9 show an instantaneous current change opposite to the direction of the voltage change of the corresponding clamp step, which may be explained by the negative slope of $i_{K_2}(V)$ in this potential range. The ratio analysis gave an open channel I–V relation of the I_x current which was essentially flat, or independent of voltage throughout the −60 to −30 mV range. The kinetics of I_x were

significantly slower than those of I_{K_2}. For example, the time constant of the current change in the left-hand panel in Fig. 9 was approximately 3 sec. We have observed even longer time constants for currents in response to clamp steps between −40 and −30 mV. The I_x activation range did not appear to be shifted by changes in K_o, although the amplitude of the current appeared to be an increasing function of K_o, as indicated by the steady-state I–V relations in Fig. 2 ($V \gtrsim -60$ mV).

Steady-state amplitude of I_{K_2} vs. K_o

The steady-state amplitudes of I_{K_2} *vs.* membrane potential are shown in Fig. 10 (lower panel) for the preparation of Fig. 2 with K_o = 1·3, 2·5, 4·8 and 6 mM. These curves were obtained by multiplying s_∞ (middle panel of Fig. 10), which was independent of K_o, and $N_s i_{K_2}(V)$ (top panel of Fig. 10). The steady-state current for $V < -100$ mV was essentially zero, regardless of the value of $N_s i_{K_2}(V)$, as all of the gates were closed in this potential range. The current also approached zero for $V \geqslant -60$ mV, even though the gates were open in this range, because of the voltage-dependent block of the channel produced by the inward rectifying process.

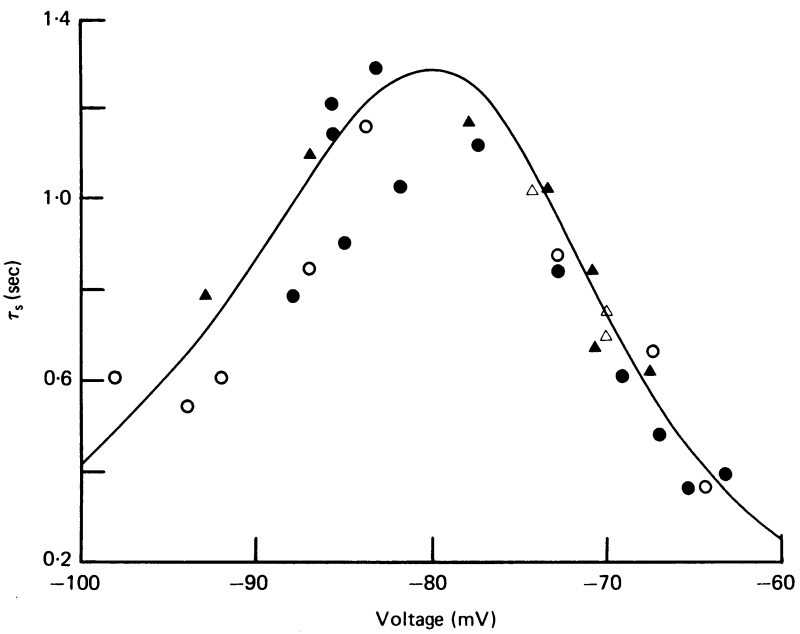

Fig. 7. Time constant of currents in response to voltage steps at K_o = 2·5 (○), 3·5 (▲), 4·8 (●), and 6·0 mM (△). Same preparation as in Fig. 2. Continuous line is best fit of $\tau_s = (\alpha+\beta)^{-1}$ with α_0 = 1·05 sec^{-1}, β_0 = 0·095 sec^{-1}, α_1 = 0·2 mV^{-1}, β_1 = 0·075 mV^{-1} and V_1 = −57 mV. Data are from a continuous impalement of the preparation.

Determination of I_{bg}

We turn now to the time-independent, or background, current $I_{bg}(V)$, which may be obtained by subtracting the steady-state I_{K_2} current in Fig. 10 from the I–V relations in Fig. 2. The results of this procedure are shown in Fig. 11*A* for K_o = 1·3, 2·5 and 6 mM. All three I–V relations inwardly rectified with a region of approximately zero slope conductance in the −90 to −70 mV range. The primary effects on I_{bg} of

elevating K_o from 1·3 to 6 mM were to reduce the slope conductance in the −100 to −80 mV range and to shift the I–V relation slightly in the outward current direction. We have modelled the I_{bg} results with three time-independent currents: an inwardly rectifying I_{K_2} current given by eqns. (1) and (2) with $r = 4$; a background sodium current $I_{Na,b}$ given by $G_{Na,b}[V - E_{Na}]$; and an outward rectifying current I_{K_4} given by $G_{K_4}(V - V_4)/1 - \exp(-k_B T(V - V_4)/e))$, which has been used by McAllister, Noble & Tsien (1975) and by Beeler & Reuter (1977) in modelling cardiac membrane action

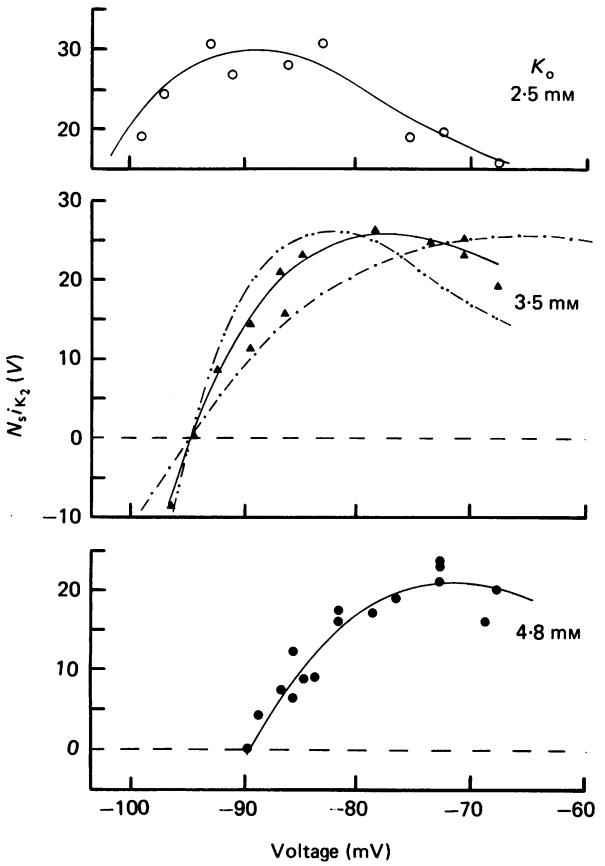

Fig. 8. Fully activated current ($N_s i_{K_2}(V)$) as a function of K_o. Same preparation as in Figs. 2 and 6. Data obtained from the I_a/I_b ratio analysis and the full distribution of I_b currents, as described in the text. Continuous lines are best fits by eye of the model of inward rectification given in eqns. (1) and (2) with $r = 2$ and $\beta = 0{\cdot}5$, $N_s e/\bar{i} = 1{\cdot}25$ μA (top), 1·09 μA (middle), 0·83 μA (bottom). Interrupted lines represent $r = 1$ (–·–) and $r = 3$ (–··–) with $\beta = 0{\cdot}5$ and $N_s e/\bar{i}$ chosen to give the same peak outward current as $r = 2$.

potentials. The internal sodium level of 7-day aggregates has been measured as 33 mM (McDonald & DeHaan, 1973), which together with Na_o = 143 mM (see Methods) gives E_{Na} = 40 mV. The other parameters of I_{K_2}, I_{K_4}, as well as $G_{Na,b}$, were adjusted (see legend of Fig. 11) to give a best fit to the I–V relation in K_o = 1·3 mM in Fig. 11*A*. The I–V relations at K_o = 2·5 and 6 mM were modelled by changing only the I_{K_2} parameters. The results of the best-fit procedure are shown in Fig. 11*B*. The $I_{bg}(V)$ model generally describes the curves in Fig. 11*A*, although the slope conductance of

the $K_o = 6$ mM model for $V \lesssim -80$ mV is somewhat lower than that of the corresponding I–V relation in Fig. 11*A*.

The theoretical curves in Fig. 11*B* coincide for $V \gtrsim -40$ mV, since the I_{K_3} component is very nearly zero for this potential range and the $I_{Na,\,b}$ and I_{K_4} currents are assumed to be independent of K_o. The I–V relations in Fig. 11*A* suggest the presence of another current component for $V \gtrsim -55$ mV, the I_x current, as previously noted in reference to Fig. 2 and Fig. 9.

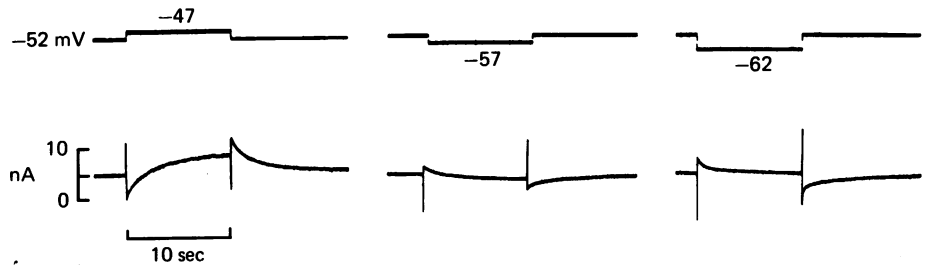

Fig. 9. Time-dependent current I_x with $K_o = 2{\cdot}5$ mM, $V_H = -52$ mV, V_{step} as indicated. The current record in the right-hand panel when V is stepped back to V_H perhaps contains a small component of inward current with rapid activation and inactivation kinetics followed by the slow I_{off} current with nearly the same amplitude as the I_{off} current in the middle panel. That is, the lower boundary of the steady-state activation curve for I_x in this preparation was approximately −55 mV. Records are filtered (low pass: 3db roll-off at 50 Hz).

DISCUSSION

Physiological significance of I_{K_2}, I_{bg} and I_x currents

The results of this paper provide a partial description of the currents responsible for spontaneous beating in heart cell aggregates. A net inward current, I_{bg}, is required to depolarize the membrane to the threshold of the TTX-sensitive current; a time-dependent current, I_{K_2}, controls the rate of pace-maker depolarization. However, other currents activated during the plateau phase of the action potential may also contribute to the rate of pace-maker depolarization. For example, Katzung & Morgenstern (1977) observed a time-dependent current lasting 100–200 sec flowing at potentials in the vicinity of the m.d.p. (−80 mV) in guinea-pig and cat papillary muscle after an induced action potential, even though these preparations do not have a time-dependent current with a steady-state activation in the subthreshold potential range. These authors attributed their findings to a mechanism similar to the I_{x_1} current of Purkinje fibres (Noble & Tsien, 1969) which is activated in papillary muscle between −30 and +20 mV. This current is not instantaneously turned off when the membrane repolarizes to the m.d.p. A similar mechanism would appear to be applicable to aggregates, since we have also observed an I_x component.

The complete determination of currents which flow during pace-making may require the results of this paper together with results obtained by imposing the voltage clamp on the aggregate at various points in time during the pace-maker depolarization, similar to the protocol used by Brown, Clark & Noble (1976*a*) and Brown, Giles & Noble (1977) in their analysis of frog atrial and sinus venosus pace-making cells.

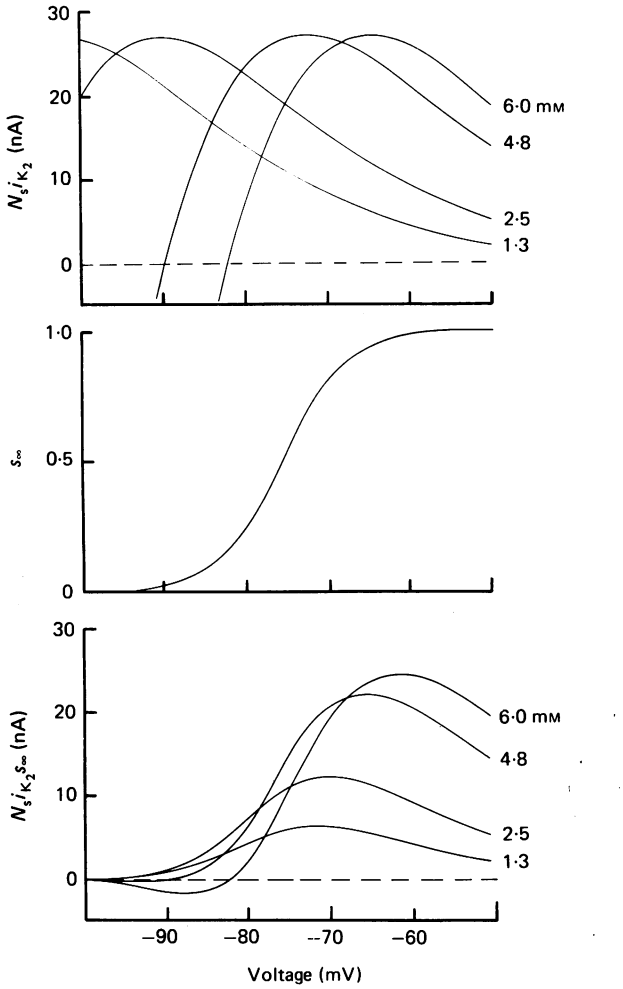

Fig. 10. Determination of the steady-state amplitude of I_{K_2}. Top panel is the theoretical description of the fully activated I_{K_2} current as described in the text and in Figs. 5*C* and 8, with $r = 2$, $\beta = 0{\cdot}5$, $N_s e/t = 1{\cdot}09\ \mu$A and K_o as given alongside each curve. The effect of changing K_o is to shift the curve along the voltage axis by the change in E_K without significantly modifying the relative amplitude of the curve, as shown by Fig. 8 in the Results. The τ_s and, consequently, the s_∞ curves (middle panel), are not affected by the changes in K_o, as shown in Fig. 7. The steady-state I_{K_2} (bottom panel) is the product of the fully activated *I–V* relation (upper panel) and the fraction of open channels which, in steady state, is given by s_∞. Consequently, the increase in steady-state I_{K_2} with increasing K_o is caused by the K_o-induced shift of the fully activated *I–V* relation into the steady-state range of activation of the s_∞ parameter.

One unambiguous role of I_{K_2} in aggregates is in the change of resting potential (E_R) when K_o was elevated from 1·3 to 2·5–6 mM. The analysis of I_{K_2} indicates that the primary cause of this effect was the change in the steady-state amplitude of I_{K_2} produced by shifting $i_{K_2}(V)$ into the range of activation of s_∞. This increase in outward current also provides a mechanism for the suppression of spontaneous beating at $K_o = 2{\cdot}5$–6 mM.

Comparison with other cardiac preparations

The most striking comparison between our results and those from other cardiac cells is the similarity of our I_{K_2} measurements with those of Noble & Tsien (1968) from mammalian Purkinje fibre. The voltage range and shape of the s_∞ activation curves for 7-day ventricular cells and Purkinje fibres appear to be virtually identical. One difference is in τ_s, which is about 2 sec maximally in Purkinje fibre as compared to 1–1·2 sec in 7-day aggregates. A second difference is in the voltage dependence of $I_{K_2}(V)$, which has its peak value about 25 mV positive to E_K in Purkinje fibre, as compared to 15 mV in 7-day aggregates. This current apparently goes away with development in the chick embryo, as shown in the succeeding paper (Clay & Shrier, 1981) and it also appears to be absent from adult ventricular preparations (Beeler & Reuter, 1977), 10–12 day chick embryo atrial cells (A. Shrier & J. R. Clay, unpublished), adult atrial tissue (Brown *et al.* 1976*a*), and sinus-venosus cells (Brown *et al.* 1977).

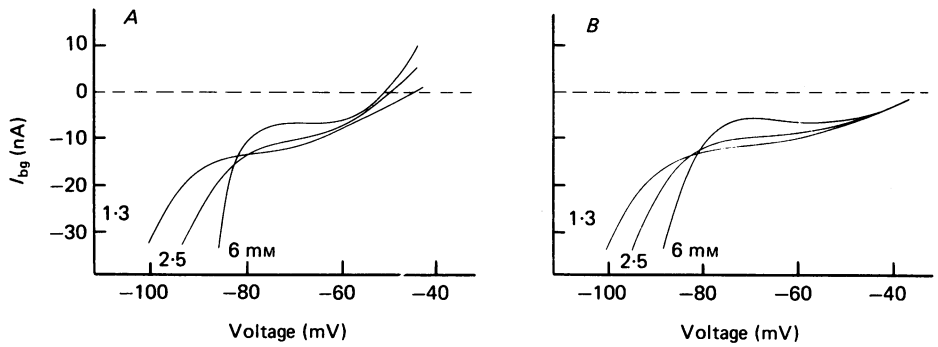

Fig. 11. Background current I_{bg} *vs.* K_o. *A*, I_{bg} obtained by subtracting the steady-state I_{K_2} current in Fig. 10 from the full steady-state *I–V* relations in Fig. 2. *B*, theoretical description of the I_{bg} results with the three-current model $I_{bg} = I_{Na,b} + I_{K_3} + I_{K_4}$, where $I_{Na,b} = G_{Na,b}(V - E_{Na})$, $I_{K_4} = G_{K_4}(V - V_4)/(1 - \exp(k_B T(V - V_4)/e))$, and I_{K_3} is the $r = 4$ form of eqns. (1) and (2). For all three curves $G_{Na,b} = 0{\cdot}0094\,\text{mS}\,.\,\text{cm}^{-2}$, $E_{Na} = 40$ mV, $G_{K_4} = 0{\cdot}024\,\text{mS}\,.\,\text{cm}^{-2}$, $V_4 = -40$ mV, and $N_3 e/t = 14{\cdot}1\,\mu\text{A}\,.\,\text{cm}^{-2}$, where N_3 is the density of I_{K_3} channels. Conductances were scaled by $A = 2{\cdot}15 \times 10^{-2}$ cm² which is calculated area for a $D = 200\,\mu$m aggregate. For $K_o = 1{\cdot}3$ mM, E_3 (the equilibrium potential for I_{K_3}) $= -95$ mV, $\beta = 0{\cdot}63$; for $K_o = 2{\cdot}5$ mM, $E_3 = -90$ mV, $\beta = 0{\cdot}58$; for $K_o = 6$ mM, $E_3 = -86$ mV, $\beta = 0{\cdot}5$.

Our measurements of time-dependent current at potentials positive to −55 mV, which we term I_x, bear some similarities to the outward repolarization currents I_{x_1} and I_{x_2} in Purkinje fibre (Noble & Tsien, 1969). The open channel *I–V* relation of I_x is similar to that of I_{x_1}, whereas the slow kinetics of I_x are rather more similar to those of I_{x_2}. A current resembling I_{x_1} appears to be a general feature of adult ventricular myocardium (Beeler & Reuter, 1970; McGuigan, 1974; Katzung & Morgenstern, 1977; McDonald & Trautwein, 1978; Cleemann & Morad, 1979), and it has also been reported in frog atrial cells (Brown, Clark & Noble, 1976*b*).

The combination of what we term I_{K_3} and I_{K_4} is similar to the time-independent I_{K_1} current in Purkinje fibre (McAllister & Noble, 1966) which has also been reported

for adult ventricular myocardium (Beeler & Reuter, 1970; McGuigan, 1974; Cleemann & Morad, 1979) and adult atrium (Noble, 1976). This current appears to be carried partly, although not exclusively, by potassium ions, since its equilibrium potential is changed by K_o somewhat less than what is predicted for a potassium electrode (Fig. 11).

The $I_{Na,b}$ current is necessary for beating to occur. In the succeeding paper we provide evidence that this current diminishes with development from a conductance ($G_{Na,b}$) of approximately 0·010 mS/cm² at 7 days to 0·003 mS/cm² at 17 days. The latter is the same value of $G_{Na,b}$ used by Beeler & Reuter (1977) in their model of the ventricular action potential. This reduction of the $I_{Na,b}$ current appears to be the primary reason for developmental loss of automaticity in ventricular aggregates.

Significance of results for whole embryonic heart

Electrophysiological measurements from intact embryonic ventricles or even small ventricular strips are difficult to interpret in terms of membrane currents, because of voltage and potassium ion inhomogeneities in the cleft spaces of these preparations. The latter may be a rather significant factor, since the membrane is sensitive to small changes in K_o (Fig. 2). Nevertheless, some qualitative connexions between our measurements and those from intact tissue may be possible.

Whole ventricle and small ventricular strips from 7-day hearts are usually quiescent with $K_o = 0$ (Carmeliet *et al.* 1976), which would appear to be inconsistent with our observations (Fig. 1). However, aggregates with diameters of several hundred μm are also quiescent in low-potassium medium. The effects of K_o on I_{K_2}, I_{K_3} and I_x may provide an explanation for this size–rate relation through the mechanism of potassium accumulation in the extracellular cleft spaces. The beat rate is independent of size for aggregates containing 1–200 cells (Clay & DeHaan, 1979), which corresponds to a 10–60 μm range of diameters. The rate is a decreasing function of size for larger preparations (Sachs & DeHaan, 1973; Clay & DeHaan, 1979) with a 50% diminution, as compared to the spontaneous beat rate of single cells, for $D = 140$ μm ($N = 2000$). Since all of the cleft spaces of a 60 μm diameter preparation are within two or three cellular layers from the external medium, accumulation may not occur to a significant degree during beating, whereas it may be a factor in the spontaneous activity of larger preparations. The effect of elevated K_o in the cleft spaces on I_{K_2} and I_{K_3} may provide an explanation for quiescence of intact tissue, since the I–V relation of these currents at elevated K_o crosses the voltage axis below threshold of the TTX-sensitive current.

The E_R measurements from aggregates and intact tissues are comparable. The apparent E_R from whole heart with $K_o = 0$ is -53 ± 2 mV (Carmeliet *et al.* 1976), which is similar to E_R in aggregates with $K_o = 1{\cdot}3$ mM and 3 μM-TTX. Moreover, the tissue E_R with $K_o = 2{\cdot}5$ mM is -80 mV, which also compares favourably with our results. As noted above, this hyperpolarization is caused by a potassium-induced increase of I_{K_2}. The tissue E_R with $K_o = 5$ mM is -70 mV (Carmeliet *et al.* 1976), whereas our measurements of E_R for $K_o = 3{\cdot}5$–6 mM were in the -80 to -75 mV range. That is, E_R displayed a U-shaped dependence on K_o both in whole tissue and in aggregates. Moreover, we observed a slight depolarization (2–3 mV) of E_R when K_o was elevated from 2·5 to 6·0 mM.

The fact that several currents flow in the subthreshold potential range may account for the variability of our measurements of E_R with K_o = 1·3 mM. Small changes of a few nA in one or more of the currents would cause a change of several mV in E_R (Fig. 2). The resting potential is less variable for K_o in the 2·5–6 mM range because the resting slope conductance is higher than it is at K_o = 1·3 mM (Fig. 2).

Potassium flux measurements from whole heart also compare favourably with our results. For example, Carmeliet *et al.* (1976) found that the labelled potassium efflux at K_o = 2·5 mM was twice as large as that at K_o = 0. As noted above, this increase of K_o hyperpolarizes E_R, and it also depolarizes E_K. Both effects reduce the driving force ($E_R - E_K$), which would appear to be inconsistent with the observed doubling of potassium efflux. However, the potassium current actually increases with hyperpolarization from −55 to −80 mV, because this potential range is on the negative slope portion of the inward rectifier for K_o = 0–2·5 mM. Flux measurements at higher levels of K_o can be interpreted in a similar manner.

Voltage and ion concentration homogeneity during measurements of I_{K_2} kinetics

Since we suggest that potassium ion accumulation may occur in the extracellular spaces of 100–200 μm diameter aggregates during the spontaneous activity of these preparations, the question of the effects of ion accumulation on our measurements of I_{K_2} kinetics naturally arises. In cardiac Purkinje fibres, where I_{K_2} is also found, accumulation is evidenced by a biphasic time-dependent current response to rectangular voltage steps in the vicinity of E_K (Baumgarten & Isenberg, 1977; DiFrancesco, 1980; DiFrancesco & Noble, 1980). That is, the concentration of potassium ions in the cleft spaces varies throughout the duration of a clamp step, which gives the appearance of time-dependent current. Consequently, a flat response when V is stepped to E_K is almost never observed, particularly at low levels of K_o (DiFrancesco & Noble, 1980). A biphasic current in the vicinity of reversal potential also obscures the interpretation of the ionic constituent of I_{K_2}, since the response appears to be consistent with potassium accumulation and an I_{K_2} mechanism consisting of the activation of an inward current on hyperpolarization (DiFrancesco & Noble, 1980).

Contrary to the results on I_{K_2} in Purkinje fibres, we have never observed a biphasic component in our current records. Moreover, our measurements of E_{eq}, such as in Fig. 6, indicate a flat current response. These results demonstrate that I_{K_2} in chick embryo heart cells is a potassium ion current and that accumulation does not occur to an observable extent during voltage-clamp steps in the subthreshold voltage range. The lack of observable effects attributable to ion accumulation appears to be due to the favourable geometry of heart cell aggregates and the small amplitude of I_{K_2} relative to currents activated during the plateau phase of the action potential.

We thank Dr R. L. DeHaan for the use of his laboratory facilities, Dr J. Pooler for the use of his HP 9810A, 9862A and 9864A computer system, and Mr T. Fisk for his technical expertise in preparing the heart cell aggregate cultures. J.R.C. was an NIH Post-doctoral Fellow. A.S. was a Post-doctoral Fellow of the Canadian Heart Foundation. This research was supported by NIH Grant 16567 to R. L. DeHaan.

REFERENCES

ADRIAN, R. H. & FREYGANG, W. H. (1962). Potassium conductance of frog muscle membrane under controlled voltage. *J. Physiol.* **163**, 104–114.

BARRY, A. (1942). Intrinsic pulsation rates of fragments of embryonic chick heart. *J. exp. Zool.* **91**, 119–130.

BAUMGARTEN, C. M. & ISENBERG, G. (1977). Depletion and accumulation of potassium in the extracellular clefts of cardiac Purkinje fibers during voltage clamp hyperpolarization and depolarization. *Pflügers Arch.* **368**, 19–31.

BEELER, G. W. & REUTER, H. (1970). Voltage clamp experiments on ventricular myocardium fibres. *J. Physiol.* **207**, 165–190.

BEELER, G. W. & REUTER, H. (1977). Reconstruction of the action potential of ventricular myocardial fibres. *J. Physiol.* **268**, 177–210.

BROWN, H. F., CLARK, A. & NOBLE, S. J. (1976*a*). Identification of the pace-maker current in frog atrium. *J. Physiol.* **258**, 521–545.

BROWN, H. F., CLARK, A. & NOBLE, S. J. (1976*b*). Analysis of pace-maker and repolarization currents in frog atrial muscle. *J. Physiol.* **258**, 547–577.

BROWN, H. F., GILES, W. & NOBLE, S. J. (1977). Membrane currents underlying activity in frog sinus venosus. *J. Physiol.* **271**, 783–816.

CARMELIET, E. E., HORRES, C. R., LIEBERMAN, M. & VEREECKE, J. S. (1976). Developmental aspects of potassium flux and permeability of the embryonic chick heart. *J. Physiol.* **254**, 673–692.

CAVANAUGH, M. W. (1955). Pulsation, migration, and division in dissociated chick embryo heart cells *in vitro*. *J. exp. Zool.* **128**, 573–589.

CLAPHAM, D. E. (1979). A whole tissue model of heart cell aggregates: electrical coupling between cells, membrane impedance, and the extracellular space. Thesis. Emory University, Atlanta, GA.

CLAY, J. R., DEFELICE, L. J. & DEHAAN, R. L. (1979). Current noise parameters derived from voltage noise and impedance in embryonic heart cell aggregates. *Biophys. J.* **28**, 169–184.

CLAY, J. R. & DEHAAN, R. L. (1979). Fluctuations in interbeat interval of rhythmic heart cell clusters; role of membrane voltage noise. *Biophys. J.* **28**, 377–390.

CLAY, J. R. & SHLESINGER, M. F. (1977). Random walk analysis of potassium fluxes associated with nerve impulses. *Proc. natn. Acad. Sci. U.S.A.* **74**, 5543–5546.

CLAY J. R. & SHRIER, A. (1981). Developmental changes in subthreshold pace-maker currents in chick embryonic heart cells. *J. Physiol.* **312**, 491–504.

CLEEMANN, L. & MORAD, M. (1979). Potassium currents in frog ventricular muscle: evidence from voltage clamp currents and extracellular potassium accumulation. *J. Physiol.* **286**, 113–143.

CONNOR, J. A. & STEVENS, C. F. (1971). Inward and delayed outward currents in isolated neural somata under voltage control. *J. Physiol.* **213**, 1–19.

DEFELICE, L. J. & DEHAAN, R. L. (1977). Membrane noise and intercellular communication. *Proc. IEEE, Special Issue Biological Signals* **65**, 796–799.

DEHAAN, R. L. (1967). Regulation of spontaneous activity and growth of embryonic chick heart cells in tissue culture. *Devl Biol.* **16**, 216–249.

DEHAAN, R. L. (1970). The potassium sensitivity of isolated embryonic heart cells increases with development. *Devl Biol.* **23**, 226–240.

DEHAAN, R. L. & FOZZARD, H. A. (1975). Membrane response to current pulses in spheroidal aggregates of embryonic heart cells. *J. gen. Physiol.* **65**, 207–222.

DIFRANCESCO, D. (1980). Evidence that i_{K_2} in Purkinje fibres is an inward current activated on hyperpolarization. *J. Physiol.* **305**, 64*P*.

DIFRANCESCO, D. & NOBLE, D. (1980). If 'i_{K_2}' is an inward current, how does it display potassium selectivity? *J. Physiol.* **305**, 14*P*.

FRANKENHAUSER, B. (1962). Potassium permeability in myelinated nerve fibres of *Xenopus laevis*. *J. Physiol.* **54**, 54–61.

GOLDMAN, D. E (1943). Potential, impedance and rectification in membranes. *J. gen. Physiol.* **27**, 37–60.

HELLAM, D. C. & STUDT, J. W. (1974). A core-conductor model of the cardiac Purkinje fibre based on structural analysis. *J. Physiol.* **243**, 637–660.

HILLE B. (1973). Potassium channels in myelinated nerve: selective permeability to small cations. *J. gen. Physiol.* **61**, 669–686.

HODGKIN, A. L. & HUXLEY, A. F. (1952*a*). Currents carried by sodium and potassium ions through the membrane of the giant axon of *Loligo*. *J. Physiol.* **116**, 449–472.

HODGKIN, A. L. & HUXLEY, A. F. (1952*b*). A quantitative description of membrane current and its application to conduction and excitation in nerve. *J. Physiol.* **117**, 500–544.

HODGKIN, A. L. & KATZ, B. (1949). The effect of sodium ions on the electrical activity of the giant axon of the squid. *J. Physiol.* **108**, 37–77.

HODGKIN, A. L. & KEYNES, R. D. (1955). The potassium permeability of a giant nerve fibre. *J. Physiol.* **128**, 61–88.

JOHNSTONE, P. N. (1925). Studies on the physiological anatomy of the embryonic heart. II. An inquiry into the development of the heart beat in chick embryos, including the development of irritability to electrical stimulation. *Bull. Johns Hopkins Hosp.* **36**, 299–311.

KATZ, B. (1949). Les constants électriques de la membrane du muscle. *Archs Sci. physiol.* **3**, 285–299.

KATZUNG, B. G. & MORGENSTERN, J. A. (1977). Effects of extracellular potassium on ventricular automaticity and evidence for a pacemaker current in mammalian ventricular myocardium. *Circulation Res.* **40**, 105–111.

MCALLISTER, R. E. & NOBLE, D. (1966). The time and voltage dependence of the slow outward current in cardiac Purkinje fibres. *J. Physiol.* **186**, 632–662.

MCALLISTER, R. E., NOBLE, D. & TSIEN, R. W. 1975). Reconstruction of the electrical activity of cardiac Purkinje fibres. *J. Physiol.* **251**, 1–59.

MCDONALD, T. F. & DEHAAN, R. L. (1973). Ion levels and membrane potential in chick heart tissue and cultured cells. *J. gen. Physiol.* **61**, 89–109.

MCDONALD, T. F. & TRAUTWEIN, W. (1978). The potassium current underlying delayed rectification in cat ventricular muscle. *J. Physiol.* **274**, 217–246.

MCGUIGAN, J. A. S. (1974). Some limitations of the double sucrose gap, and its use in a study of the slow outward current in mammalian ventricular muscle. *J. Physiol.* **240**, 775–806.

MATHAN, R. D. & DEHAAN, R. L. (1979). Voltage clamp analysis of embryonic heart cell aggregates. *J. gen. Physiol.* **73**, 175–198.

NEHER, E. & STEVENS, C. F. (1977). Conductance fluctuations and ionic pores in membranes. *A. Rev. Biophys. Bioeng.* **6**, 345–381.

NOBLE, D. (1975). *The Initiation of the Heartbeat*. London: Oxford University Press.

NOBLE, S. J. (1976). Potassium accumulation and depletion in frog atrial muscle. *J. Physiol.* **258**, 579–613.

NOBLE, D. TSIEN, R. W. (1968). The kinetics and rectifier properties of the slow potassium current in cardiac Purkinje fibres. *J. Physiol.* **195**, 185–214.

NOBLE, D. & TSIEN, R. W. (1969). Outward currents activated in the plateau range of potentials in cardiac Purkinje fibres *J. Physiol.* **200**, 205–231.

PATTEN, B. M. & KRAMER, T. C. (1933). The initiation of contraction in the embryonic chick heart. *Am. J. Anat.* **53**, 349–375.

SABIN, F. R. (1917). Origin and development of the primitive vessels of the chick and of the pig. *Carnegie Contrib. Embryol.* **9**, 213–264.

SACHS, H. G. & DEHAAN, R. L. (1973). Embryonic myocardial cell aggregates; volume and pulsation rate. *Devl Biol.* **30**, 233–240.

SHRIER, A. & CLAY, J. R. (1980). Pacemaker currents in embryonic chick heart cells change with development. *Nature, Lond.* **283**, 670–671.

TASAKI, I. (1955). New measurements of the capacity and the resistance of the myelin sheath and the nodal membrane of the isolated frog nerve fiber. *Am. J. Physiol.* **181**, 639–650.

VAN MIEROP, L. H. S. (1967). Location of pacemaker in chick embryo heart at the time of initiation of heartbeat. *Am. J. Physiol.* **212**, 407–415.